J. Comp. App. Res. Mech. Eng. Vol. X. No. X, pp. X-X, XXXX DOI: 10.22061/jcarme.XXXX.XXXX.XXXX

SRTTU Journal of Computational and Applied Research in Mechanical Engineering jcarme.sru.ac.ir JCARME ISSN: 2228-7922

Research paper

# Accurate diagnosis of mechanical faults in a single-phase AC electromotor through acoustic monitoring and machine learning techniques

**V. Samadi [a], M. Mostafaei [a, b]* and A. N. Lorestani [a]**

[a] *Department of Mechanical Engineering of Biosystems, Razi University, Kermanshah, Iran*
[b] *Department of Biosystems Engineering, University of Tabriz, Tabriz, Iran*

**Article info:**

**Article history:**

| | |
|---|---|
| Received: | 00/00/0000 |
| Revised: | 00/00/0018 |
| Accepted: | 00/00/0000 |
| Online: | 00/00/0000 |

**Keywords:**
Acoustic signals,
Classification,
Electromotor,
Fault detection,
Machine learning.

***Corresponding author:**
b.mostafaei@tabrizu.ac.ir

**Abstract**

This study presents a non-invasive method for detecting mechanical faults in a single-phase AC electromotor using processed acoustic signals. Sound data were collected via a USB-connected microphone installed in the motor's electrical casing under diverse operating conditions. Ten statistical features were extracted from the acoustic signals and used as input to three classification algorithms: Linear Discriminant Analysis (LDA), Quadratic Discriminant Analysis (QDA), and Support Vector Machine (SVM). Model performance was evaluated using confusion matrix metrics, including specificity, accuracy, precision, and sensitivity. Among the classifiers, SVM outperformed others, achieving average values of 99.5, 99.2, 97.1, and 96.7, respectively. The findings confirm that acoustic signal analysis is a reliable and cost-effective tool for real-time fault diagnosis in electromotors. Defects may be accurately found in the electromotor by using acoustic analysis to monitor its status. The proposed framework is adaptable to other rotating machinery through retraining, offering a valuable solution for predictive maintenance in industrial applications.

## 1. Introduction

To avoid significant faults in engineering systems, several researchers have looked at error detection and preventive maintenance in recent years. Numerous factors, including vibration, sound, and temperature, have been taken into account while analyzing machine failures. It is possible to evaluate the operational state of machines, which are often inaccessible, by using external data. Signal analysis is one of the most useful instruments that engineers and researchers have thought of [1].

One of the most widely used components in the industry is the electromotor, which is available in many forms. A breakdown of an electromotor in an industrial unit may cause the work to stop and increase the cost of repairs. Timely detection and repair of various defects in the electromotor prevents it from stopping suddenly and stopping the work process. In the usual method, this operation may cause more costs due to the lack of a correct and early diagnosis of the defect. Therefore, new methods of fault diagnosis and monitoring the condition of machines can help to accurately diagnose the type of damage promptly and save on various costs. Today, employing sound analysis to monitor the condition of rotating industrial equipment is one way to reduce the cost of maintenance and repair. There could be differences in the health and failure states of the sound signals coming from various electromotor components [2].

So far, numerous techniques have been employed in machine troubleshooting, such as the use of acoustic emission techniques in internal combustion engines [3], current signal analysis for gearbox fault detection in induction motors [4, 5], and regular and continuous vibration and compressor noise measurement in internal combustion engine fault diagnosis [6].

Another study also investigated the early detection of defects in a single-phase electromotor using acoustic signals. The electromotor's conditions—healthy, with faulty bearings, and with both faulty bearings and a coil connection—were measured and examined by the authors [7].

In another study, Messi Ferguson's tractor starter motor fault was intelligently detected using vibration monitoring and an adaptive neuro-fuzzy inference system (ANFIS). Vibration data were collected from the starter motor in health and failure conditions using a piezoelectric accelerometer sensor and a data-driven system. The results of classification with a confusion matrix showed that the accuracy of detection with this method was appropriate [8].

A study has proposed the Fourier decomposition method (FDM) for fault detection based on acoustic signals for planetary gearboxes. The results showed that the accuracy of error detection in this proposed method reaches 96.32%, which achieved a better fault detection effect compared to vibration signals [9]. In a research, electric locomotive bearing fault diagnosis was presented through a convolutional deep belief network (CDBN) with Gaussian visible units to learn the high-layer features. The proposed method was applied to the analysis of experimental signals collected for automatic and accurate identification of electric locomotive bearing faults [10]. Table 1 summarizes the numbers of studies discussed herein.

Linear discriminant analysis (LDA) is a statistical method used in machine learning and pattern recognition to find the linear combination of properties that best distinguishes two or more classes of objects. The LDA method maximizes intergroup variance and minimizes intragroup variance in order to optimize segregation between groups. It is based on the assumption that each class can be modeled by a Gaussian distribution and that all the classes share the same covariance matrix. Quadratic discriminant analysis (QDA) is similar to LDA but without the assumption that the classes share the same covariance matrix, i.e., each class has its own covariance matrix. In this case, the boundary between classes is a quadratic surface instead of a hyperplane [11, 12].

A support vector machine (SVM) is one of the supervised learning methods used for classification and regression. The SVM algorithm is classified as a pattern recognition algorithm. This algorithm can be used wherever there is a need to identify patterns or classify objects in specific classes. SVM Classifier is based on linear data classification, and in this division, it tries to choose a line that has a more confident margin [13, 14].

In parallel with the advancement of machine learning techniques in engineering diagnostics, Artificial Neural Networks (ANNs) have demonstrated remarkable success across various mechanical engineering domains. For instance, in a recent comprehensive study by Sekban et al. (2024), the formability behavior of friction stir-welded high-strength AH32 shipbuilding steel was investigated using an integrated approach of experimental methods, finite element analysis, and ANNs. Their research confirmed that ANN models could achieve extremely consistent results with experimental data, highlighting the capability of such data-driven models to accurately predict complex mechanical behaviors even in the absence of extensive experimental studies. This underscores the broader potential and reliability of machine learning methods, including ANNs, for solving intricate problems in mechanical system analysis and fault diagnosis [20].

**Table 1.** Summary of relevant studies on fault diagnosis methods.

| Subject | Method | Result | Reference |
|---|---|---|---|
| Investigation of engine fault diagnosis | Discrete wavelet transforms and neural network | Sound emission signal can be used for fault diagnosis of various engine operating conditions. | [15] |
| Fault detection and diagnosis of an industrial steam turbine | SVM (Support vector machine) and ANFIS (Adaptive neuro-fuzzy inference system) | The experimental operation of the SVM classifier was better than the ANFIS classifier operation through a fusion strategy. | [16] |
| Fault conditions classification of automotive generator | ANFIS | The proposed system has potential in fault diagnosis of the automotive generator | [17] |
| Assessment of gearbox fault detection | Vibration signal analysis and acoustic emission technique | Vibration signature analysis and acoustic emission are two very efficient techniques for early fault detection. | [5] |
| Fault classification of a kind of clutch mechanism retainer | Vibration analysis using the ANFIS | Total classification accuracy was 100% in all models. | [18] |
| Fault detection of bearings and stators in a single-phase induction motor | Sound analysis and machine learning methods | Total efficiency of acoustic signal recognition for three classifiers of nearest neighbor, nearest mean and gaussian mixture were 91.6, 95.3, and 88.8, respectively. | [7] |
| Fault diagnosis of rotating electrical machines | Vibration analysis and machine learning methods and the application of multiple classifications | The possibility of electromotor fault detection. | [19] |
| Fault detection based on acoustic signals for planetary gearboxes | Fourier decomposition method (FDM) | The accuracy of error detection reaches 96.32% and better than vibration signals. | [9] |

While LDA, QDA, and SVM are established classification methods, the novelty of this work lies in their integrated application to develop a cost-effective and non-invasive diagnostic framework. This framework successfully discriminates between multiple concurrent mechanical faults (bearing failure, shaft imbalance, and shaft wear) in a single-phase AC motor using only commercially available acoustic sensors, demonstrating a practical and accessible alternative to vibration-based monitoring for industrial settings. The performance of the proposed approaches was rigorously evaluated using confusion matrix metrics, including sensitivity, specificity, precision, and accuracy. Although based on a laboratory test bench, the methodology shows strong potential for generalization to other rotating machinery through model retraining.

## 2. Materials and methods

This research was performed on a single-phase low-power AC electromotor MOTOGEN TABRIZ-IRAN with an output power of 1.1 kW, rated voltage of 220 V, speed in the rated load of 1420 rpm, rated current of 7.4 A, and rated torque of 7.4 N.m. Sound waves were measured at WAV format using a YW-001 wired sound microphone with a frequency range of 15-30 kHz, impedance of 2.2 kΩ, and sensitivity of 52±5 dB, which was connected to a laptop through the USB interface. The sensor was placed in the electrical circuit housing (distribution box) of the electromotor. An RM-1501 laser tachometer was also utilized to measure the rotation speed of the electromotor (Fig. 1).

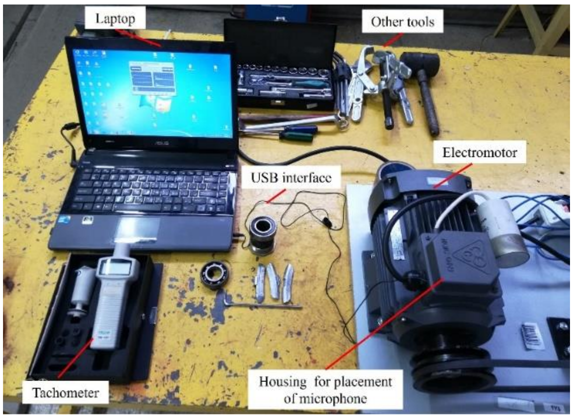


**Fig. 1.** Experimental tools and equipment.

The present study was performed to detect and identify common mechanical defects of an AC single-phase electromotor (including bearing failure, shaft imbalance, and shaft surface wear), at two common operating speeds (500 and 1400 rpm) by processing acoustic signals. Acoustic data were collected using the sound card of a laptop device and the application of the AD Sound Recorder software. According to Fig. 2, data were collected from one healthy condition (H) and three separate electromotor failure modes, including bearing failure (FB), shaft unbalance (USH), and shaft surface wear (WSH). The number of electromotor rotation speeds, total number of test modes, and repetitions of the tests were 2 (500 and 1400 rpm), 4 modes (H, FB, USH, and WSH), and 30 times, resulting in a total of 240 data points (2 × 4 × 30). In this study, the failures were in the form of damage and wear of the inner ring of the bearing, reduction of the shaft diameter by 10%, and unbalance using a 20 g load (Fig. 2).

## *2.1. Signal processing*

Signal processing is one of the most important and widely used topics in engineering fields. Signal processing was performed using the tools in the MATLAB software digital processing toolbox to convert analog signals in the time domain to digital data in the frequency domain. In order to process the received acoustic signals, they must be intelligible to the computer (digital signals only). Because the microphone output was an analog output, it could not enter the computer system directly; Therefore, connect the microphone to the laptop sound card, and the signals were recorded and stored in each of the health and failure modes. An example of the electromotor sound spectrum is illustrated in Fig. 3 (USH mode and 1400 rpm).
Audio signal processing refers to the purposeful transformation of acoustic data, usually done by Audio Effects or Audio Units. Since it is possible to display audio signals in both digital and analog formats, signal processing is possible in both areas. Analog processors operate directly on electronic signals, while digital processors mathematically operate on a digital instance of that signal.

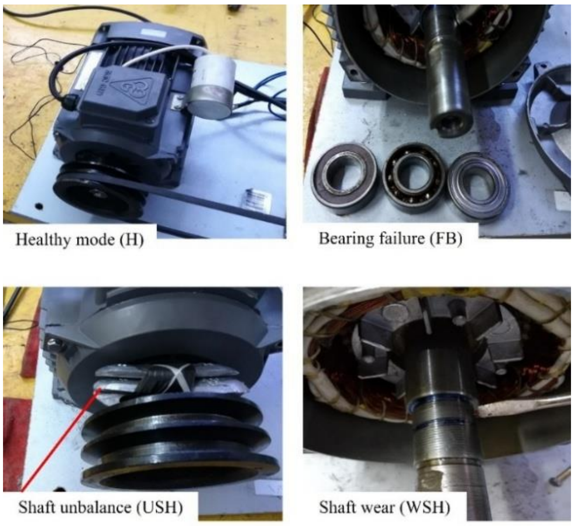


**Fig. 2.** Electromotor failure modes.

The processed signals were used to extract ten normalized statistical characteristics under both healthy and defective conditions.

## *2.2. Calculation of statistical characteristics*

The feature vector that is selected as the network input represents a summary of the most important problem properties for identifying and classifying faults. The most important properties were calculated using some time and frequency domain parameters. Ten statistical characteristics of audio signals were calculated according to Table 2 [8]. Each of these properties was calculated using the corresponding formulas. Before using the statistical properties in the classification algorithm, they were normalized to have a uniform effect on the algorithm.

## *2.3. Classification of defects*

After data collection and signal processing, the data were sorted into the states of healthy and failure modes by different approaches of LDA, QDA, and SVM. In the present study, 70% of the obtained data were used for model training, and 30% for testing and evaluation. The inputs of the models included the calculated characteristics, and the outputs were different modes of the electromotor (Fig. 4).

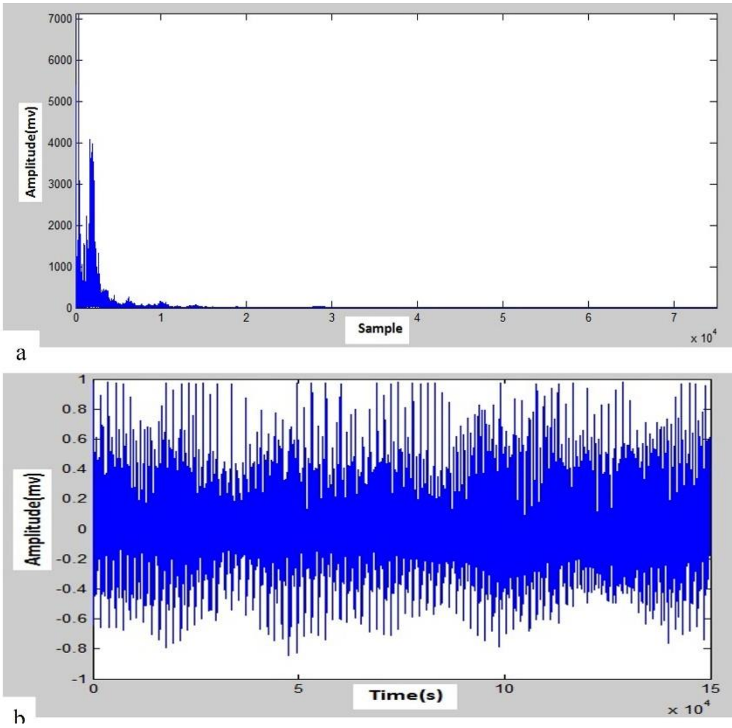


**Fig. 3.** Frequency spectrum (a), time spectrum (b) of electromotor acoustic signals in USH mode and 1400 rpm.

**Table 2.** Calculated statistical properties.

| Property description | A1 mean | A2 median | A3 Std. deviation | A4 variance | A5 skewness |
|---|---|---|---|---|---|
| Formula | $\frac{1}{n}\sum x_i$ | $\frac{X_{\frac{n}{2}} + X_{\frac{n}{2}+1}}{2}$ | $\sqrt{\frac{1}{n}\sum (x_i - \bar{x})^2}$ | $\frac{\sum (x_i - \bar{x})^2}{n-1}$ | $\frac{(n)}{(n-1)(n-2)}\sum\left(\frac{x_i - \bar{x}}{s}\right)^3$ |
| Property description | A6 kurtosis | A7 range | A8 minimum | A9 maximum | A10 sum |
| Formula | $\frac{1}{n}\sum\left(\frac{x_i - \bar{x}}{s}\right)^4$ | $\mathrm{Max}\,(x) - \mathrm{Min}\,(x)$ | $x_0 \leq x$ | $x_0 \geq x$ | $\sum x_i$ |

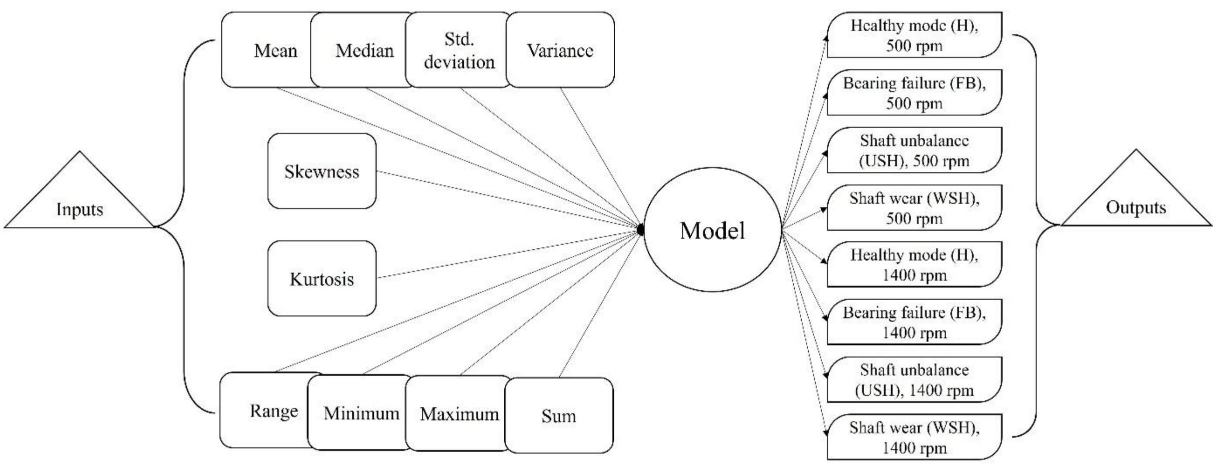


**Fig. 4.** Inputs and outputs of classification models.

The analysis obtained from the confusion matrix gave rise to four states of true positive (TP) or hit, true negative (TN) or correct rejection, false positive (FP) or underestimation, and false negative (FN) equivalent with miss or overestimation. The unscrambler X10.4 software was used for LDA, QDA, and SVM analyses after preprocessing the data.
Parameters such as sensitivity, specificity, precision, and accuracy (Eqs. 1-4) were used to analyze the performance of classifier models [21].

$$\text{Sensitivity} = \frac{\text{TP}}{\text{TP} + \text{FN}} \times 100 \quad (1)$$

$$\text{Specificity} = \frac{\text{TN}}{\text{TN} + \text{FP}} \times 100 \quad (2)$$

$$\text{Precision} = \frac{\text{TP}}{\text{TP} + \text{FP}} \times 100 \quad (3)$$

$$\text{Accuracy} = \frac{\text{TP} + \text{TN}}{\text{TP} + \text{TN} + \text{FN} + \text{FP}} \times 100 \quad (4)$$

## 3. Results and discussion

### *3.1. Results of linear discriminant analysis (LDA)*

In the present study, the LDA method was one of the methods used to diagnose and classify electromotor defects in 8 classes (H500, FB500, USH500, WSH500, H1400, FB1400, USH1400, and WSH1400). Each class had 30 replications, so 21 replications (70% of the data) were used randomly to train the model, and 9 replications (30% of the data) were used to evaluate and test it. The results of the confusion matrix (Table 3) showed that in the linear discriminant analysis, only 5 data points out of 168 training data were mistakenly placed in another group, and 4 data points from the test data were similar. The calculation of the performance parameters of this model is presented in Table 4. The findings indicated that the mean of accuracy, precision, specificity, and sensitivity for the whole data were 99.1, 96.6, 99.5, and 96.2, respectively. These results show the high reliability and accuracy of this model in the separation and classification of defects related to the electromotor. The weakest classifications were related to the USH1400 and WSH1400 classes. The precision of the USH1400 class and the sensitivity of the WSH1400 class for all data were 80.6 and 80.0, respectively. Due to the high rotational speed of the electromotor and the similarity of acoustic signals in these two classes, the model's performance declines under such conditions.
Fig. 5 shows an example of classifying training data for different types of electromotor modes using the LDA approach. The plot visualizes the distribution of different classes in the two-dimensional discriminant space, with LD1 (First Linear Discriminant) and LD2 (Second Linear Discriminant) as the coordinate axes.

**Table 3.** Confusion matrix of the LDA model.

| Data type | Classes | H500 | FB500 | USH500 | WSH500 | H1400 | FB1400 | USH1400 | WSH1400 |
|---|---|---|---|---|---|---|---|---|---|
| Training data | H500 | 21 | 0 | 0 | 0 | 0 | 0 | 0 | 0 |
| | FB500 | 0 | 21 | 0 | 0 | 0 | 0 | 0 | 0 |
| | USH500 | 0 | 0 | 21 | 0 | 0 | 0 | 0 | 0 |
| | WSH500 | 0 | 0 | 0 | 21 | 0 | 0 | 0 | 0 |
| | H1400 | 0 | 0 | 0 | 0 | 20 | 0 | 0 | 0 |
| | FB1400 | 0 | 0 | 0 | 0 | 0 | 20 | 0 | 0 |
| | USH1400 | 0 | 0 | 0 | 0 | 1 | 0 | 20 | 2 |
| | WSH1400 | 0 | 0 | 0 | 0 | 0 | 1 | 1 | 19 |
| Testing data | H500 | 9 | 0 | 0 | 0 | 0 | 0 | 0 | 0 |
| | FB500 | 0 | 9 | 0 | 0 | 0 | 0 | 0 | 0 |
| | USH500 | 0 | 0 | 9 | 0 | 0 | 0 | 0 | 0 |
| | WSH500 | 0 | 0 | 0 | 9 | 0 | 0 | 0 | 0 |
| | H1400 | 0 | 0 | 0 | 0 | 9 | 0 | 0 | 0 |
| | FB1400 | 0 | 0 | 0 | 0 | 0 | 9 | 0 | 0 |
| | USH1400 | 0 | 0 | 0 | 0 | 0 | 0 | 9 | 4 |
| | WSH1400 | 0 | 0 | 0 | 0 | 0 | 0 | 0 | 5 |

**Table 4.** Performance parameters of the LDA model.

| Data type | Classes/ Parameters | TP | FP | FN | TN | Specificity | Accuracy | Precision | Sensitivity |
|---|---|---|---|---|---|---|---|---|---|
| | H500 | 21 | 0 | 0 | 147 | 100.0 | 100.0 | 100.0 | 100.0 |
| | FB500 | 21 | 0 | 0 | 147 | 100.0 | 100.0 | 100.0 | 100.0 |
| | USH500 | 21 | 0 | 0 | 147 | 100.0 | 100.0 | 100.0 | 100.0 |
| | WSH500 | 21 | 0 | 0 | 147 | 100.0 | 100.0 | 100.0 | 100.0 |
| Training | H1400 | 20 | 0 | 1 | 147 | 100.0 | 99.4 | 100.0 | 95.2 |
| | FB1400 | 20 | 0 | 1 | 147 | 100.0 | 99.4 | 100.0 | 95.2 |
| | USH1400 | 20 | 3 | 1 | 144 | 98.0 | 97.6 | 87.0 | 95.2 |
| | WSH1400 | 19 | 2 | 2 | 145 | 98.6 | 97.6 | 90.5 | 90.5 |
| | | | | | **Ave.** | **99.6** | **99.3** | **97.2** | **97.0** |
| | H500 | 9 | 0 | 0 | 63 | 100.0 | 100.0 | 100.0 | 100.0 |
| | FB500 | 9 | 0 | 0 | 63 | 100.0 | 100.0 | 100.0 | 100.0 |
| Testing | USH500 | 9 | 0 | 0 | 63 | 100.0 | 100.0 | 100.0 | 100.0 |
| | WSH500 | 9 | 0 | 0 | 63 | 100.0 | 100.0 | 100.0 | 100.0 |
| | H1400 | 9 | 0 | 0 | 63 | 100.0 | 100.0 | 100.0 | 100.0 |
| | FB1400 | 9 | 0 | 0 | 63 | 100.0 | 100.0 | 100.0 | 100.0 |
| | USH1400 | 9 | 4 | 0 | 59 | 93.7 | 94.4 | 69.2 | 100.0 |
| | WSH1400 | 5 | 0 | 4 | 63 | 100.0 | 94.4 | 100.0 | 55.6 |
| | | | | | **Ave.** | **99.2** | **98.6** | **96.2** | **94.4** |
| | H500 | 30 | 0 | 0 | 210 | 100.0 | 100.0 | 100.0 | 100.0 |
| | FB500 | 30 | 0 | 0 | 210 | 100.0 | 100.0 | 100.0 | 100.0 |
| All data | USH500 | 30 | 0 | 0 | 210 | 100.0 | 100.0 | 100.0 | 100.0 |
| | WSH500 | 30 | 0 | 0 | 210 | 100.0 | 100.0 | 100.0 | 100.0 |
| | H1400 | 29 | 0 | 1 | 210 | 100.0 | 99.6 | 100.0 | 96.7 |
| | FB1400 | 29 | 0 | 1 | 210 | 100.0 | 99.6 | 100.0 | 96.7 |
| | USH1400 | 29 | 7 | 1 | 203 | 96.7 | 96.7 | 80.6 | 96.7 |
| | WSH1400 | 24 | 2 | 6 | 208 | 99.0 | 96.7 | 92.3 | 80.0 |
| | | | | | **Ave.** | **99.47 ± 1.47** | **98.62±1.77** | **96.61±7.7** | **95.84±9.6** |

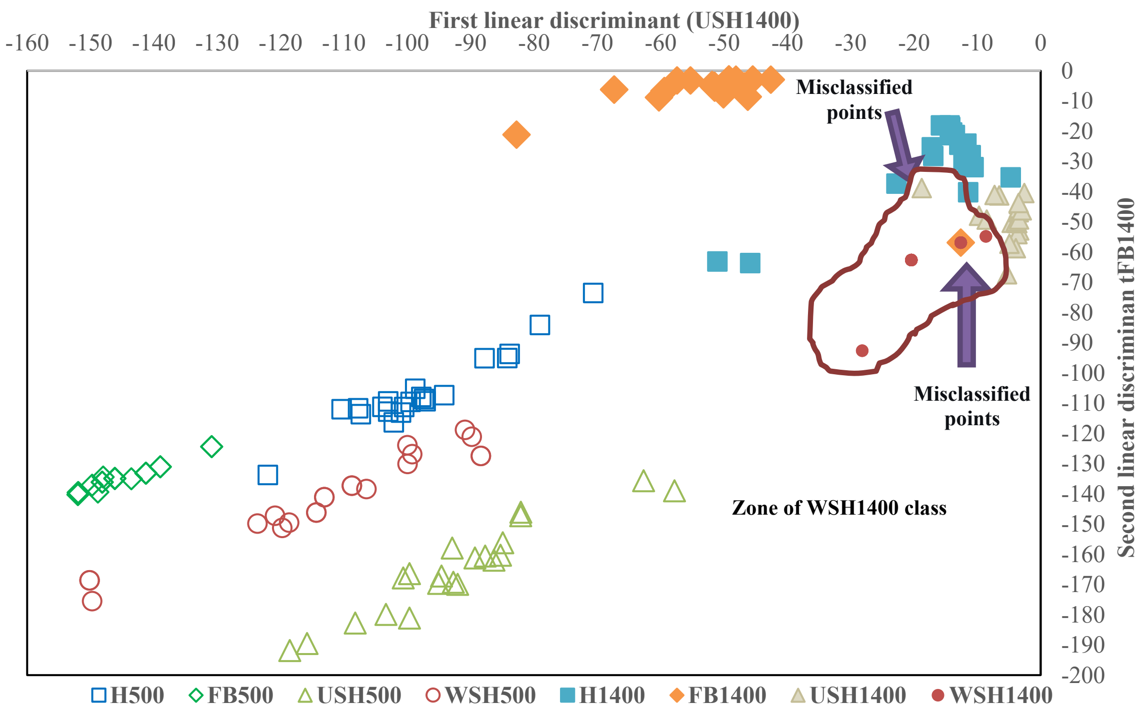


**Fig. 5.** The classification plot of the linear discriminant analysis approach.

As verified by the confusion matrix in Table 3, specific misclassification patterns are visually identifiable: certain samples from both FB1400 and USH1400 classes are erroneously clustered within the WSH1400 region. These misclassified instances are explicitly marked with distinct symbols for clarity. The remaining correctly classified WSH1400 samples in this area demonstrate appropriate clustering, indicating regions of feature space overlap between classes that present classification challenges for the LDA model.

In a study comparing the audio signals processed from gearbox gears in healthy and defective conditions, it was shown that the effect of the defect type can be seen by increasing the frequency range and its harmonics or creating sub-bands around the gear engagement frequency [2]. Also, in another study, using the obtained sound data and employing the decision tree algorithm, a model was developed to learn and classify the bearing condition. The inputs of the model were statistical parameters such as mean, median, and kurtosis. The model accuracy was 95.5% for classifying bearing conditions [22].

### 3.2. Results of quadratic discriminant analysis (QDA)

In the QDA model, each class had 30 replications, so 21 replications (70% of the data) were used randomly to train the model, and 9 replications (30% of the data) were used to evaluate and test it. The results of data analysis of electromotor defects at different rotational speeds using the QDA approach are presented in Table 5. The results showed that in all classifications, the detection of acoustic signals related to USH500, WSH500, and H1400 was performed with complete accuracy and precision. The findings also indicated that the QDA approach had no sensitivity to the acoustic signals of the WSH1400 class, and all the signals of this class were mistakenly placed in other classes. Therefore, its sensitivity and precision in the training and testing data were zero, as well as all data. In this classification, all data related to the WSH1400 class were misclassified into the USH1400 or FB1400 classes. Consequently, the QDA approach demonstrated lower average precision and sensitivity compared to the LDA method.

The complete failure of QDA in classifying WSH1400 samples (0% sensitivity/precision) reveals a key limitation of our feature set. It can be said that most likely, both shaft unbalance (USH) and wear (WSH) primarily excite 1x rotational frequency and harmonics at high speeds, making them spectrally similar. Our general statistical features, while effective for broader classification, cannot capture the subtle differences between these specific fault signatures. This finding clearly indicates the need for more specialized features (e.g., harmonic ratios, sideband analysis) to discriminate between mechanically different but spectrally similar faults.

In a recent paper published by the present authors, similar results were obtained using similar data and a machine learning method for the detection and classification of electromotor defects. The results showed final classification sensitivity of 95.63% and an overall classification accuracy of 95.71% [23].

The performance drop observed in challenging classes like WSH1400 and USH1400 underscores the limitation of using a simple train-test split with limited data. While the 70/30 split provided initial performance estimates, this validation approach may introduce statistical variability due to the limited sample size per class. Employing k-fold cross-validation in future studies could yield more robust and reliable performance metrics by utilizing the entire dataset more effectively for both training and validation.

### 3.3. Results of support vector machine (SVM)

In the SVM model, each class had 30 replications, so 21 replications (70% of the data) were used randomly to train the model, and 9 replications (30% of the data) were used to evaluate and test it. To use the SVM approach, data were first entered into the software to train it, and the optimal model settings were obtained from its grid search capability as follows: SVM type of classification (nu-SVC), kernel type of polynomial degree 2, gamma of 0.1, offset of 0, nu value of 0.255, and input weights of 1.

**Table 5.** Performance parameters of the QDA model.

| Data type | Classes/ Parameters | TP | FP | FN | TN | Specificity | Accuracy | Precision | Sensitivity |
|---|---|---|---|---|---|---|---|---|---|
| | H500 | 21 | 0 | 0 | 147 | 100.0 | 100.0 | 100.0 | 100.0 |
| | FB500 | 21 | 0 | 0 | 147 | 100.0 | 100.0 | 100.0 | 100.0 |
| | USH500 | 21 | 0 | 0 | 147 | 100.0 | 100.0 | 100.0 | 100.0 |
| | WSH500 | 21 | 0 | 0 | 147 | 100.0 | 100.0 | 100.0 | 100.0 |
| Training data | H1400 | 21 | 0 | 0 | 147 | 100.0 | 100.0 | 100.0 | 100.0 |
| | FB1400 | 21 | 17 | 0 | 130 | 88.4 | 89.9 | 55.3 | 100.0 |
| | USH1400 | 21 | 4 | 0 | 143 | 97.3 | 97.6 | 84.0 | 100.0 |
| | WSH1400 | 0 | 0 | 21 | 147 | 100.0 | 87.5 | 00.0 | 00.0 |
| | | | | | **Ave.** | **98.2** | **96.9** | **79.9** | **87.5** |
| | H500 | 9 | 8 | 0 | 55 | 87.3 | 88.9 | 52.9 | 100.0 |
| | FB500 | 1 | 0 | 8 | 63 | 100.0 | 88.9 | 100.0 | 11.1 |
| Testing data | USH500 | 9 | 0 | 0 | 63 | 100.0 | 100.0 | 100.0 | 100.0 |
| | WSH500 | 9 | 0 | 0 | 63 | 100.0 | 100.0 | 100.0 | 100.0 |
| | H1400 | 9 | 0 | 0 | 63 | 100.0 | 100.0 | 100.0 | 100.0 |
| | FB1400 | 9 | 5 | 0 | 58 | 92.1 | 93.1 | 64.3 | 100.0 |
| | USH1400 | 9 | 4 | 0 | 59 | 93.7 | 94.4 | 69.2 | 100.0 |
| | WSH1400 | 0 | 0 | 9 | 63 | 100.0 | 87.5 | 00.0 | 00.0 |
| | | | | | **Ave.** | **96.6** | **94.1** | **73.3** | **76.4** |
| | H500 | 30 | 8 | 0 | 202 | 96.2 | 96.7 | 78.9 | 100.0 |
| | FB500 | 22 | 0 | 8 | 210 | 100.0 | 96.7 | 100.0 | 73.3 |
| All data | USH500 | 30 | 0 | 0 | 210 | 100.0 | 100.0 | 100.0 | 100.0 |
| | WSH500 | 30 | 0 | 0 | 210 | 100.0 | 100.0 | 100.0 | 100.0 |
| | H1400 | 30 | 0 | 0 | 210 | 100.0 | 100.0 | 100.0 | 100.0 |
| | FB1400 | 30 | 22 | 0 | 188 | 89.5 | 90.8 | 57.7 | 100.0 |
| | USH1400 | 30 | 8 | 0 | 202 | 96.2 | 96.7 | 78.9 | 100.0 |
| | WSH1400 | 0 | 0 | 30 | 210 | 100.0 | 87.5 | 00.0 | 00.0 |
| | | | | | **Ave.** | **97.74±4.16** | **96.02±4.98** | **76.95±33.86** | **84.17±36.96** |

The performance parameters of the SVM approach for the detection and classification of the electromotor defects in the three statuses of train, test, and all data are presented in Table 6. As can be seen, the most classification errors occurred in the WSH1400 and USH1400 classes and caused a downward trend for their precision and sensitivity parameters, especially in the test data. Four out of nine test data for WSH1400 are incorrectly placed in USH1400, so the precision for USH1400 class test data dropped sharply to the lowest value of 69.2. The sensitivity parameter was also estimated to be at its lowest value of 55.6 for the WSH1400 class due to the incorrect classification of some test data. The calculations of performance parameters for other classes show high accuracy. In the SVM approach, the average of specificity, accuracy, precision, and sensitivity for all data was calculated to be 99.5, 99.2, 97.1, and 96.7, respectively. An example of an SVM approach classification plot for training data is shown in Fig. 6. In the Support Vector Machine (SVM) decision boundary projection plot, the distribution pattern of data points in the two-dimensional space clearly reveals misclassification cases. As illustrated in the figure, one sample from class FB1400 is incorrectly positioned within the region belonging to class WSH1400. Three samples from other classes are also erroneously located within the USH1400 class boundary. This unexpected dispersion of samples into other classes' territories directly corresponds with the values in the confusion matrix (Table 5). The position of these points in the projected space indicates that the extracted features of these particular samples have values that align more closely with the decision boundaries of other classes according to the SVM model. .

**Table 6.** Performance parameters of the SVM model.

| Data type | Classes/ Parameters | TP | FP | FN | TN | Specificity | Accuracy | Precision | Sensitivity |
|---|---|---|---|---|---|---|---|---|---|
| | H500 | 21 | 0 | 0 | 147 | 100.0 | 100.0 | 100.0 | 100.0 |
| | FB500 | 21 | 0 | 0 | 147 | 100.0 | 100.0 | 100.0 | 100.0 |
| | USH500 | 21 | 0 | 0 | 147 | 100.0 | 100.0 | 100.0 | 100.0 |
| | WSH500 | 21 | 0 | 0 | 147 | 100.0 | 100.0 | 100.0 | 100.0 |
| Training data | H1400 | 20 | 0 | 1 | 148 | 100.0 | 99.4 | 100.0 | 95.2 |
| | FB1400 | 20 | 0 | 1 | 148 | 100.0 | 99.4 | 100.0 | 95.2 |
| | USH1400 | 21 | 3 | 0 | 144 | 98.0 | 98.2 | 87.5 | 100.0 |
| | WSH1400 | 19 | 1 | 2 | 148 | 99.3 | 98.2 | 95.0 | 90.5 |
| | | | | | **Ave.** | **99.7** | **99.4** | **97.8** | **97.6** |
| | H500 | 9 | 0 | 0 | 63 | 100.0 | 100.0 | 100.0 | 100.0 |
| | FB500 | 9 | 0 | 0 | 63 | 100.0 | 100.0 | 100.0 | 100.0 |
| Testing data | USH500 | 9 | 0 | 0 | 63 | 100.0 | 100.0 | 100.0 | 100.0 |
| | WSH500 | 9 | 0 | 0 | 63 | 100.0 | 100.0 | 100.0 | 100.0 |
| | H1400 | 9 | 0 | 0 | 63 | 100.0 | 100.0 | 100.0 | 100.0 |
| | FB1400 | 9 | 0 | 0 | 63 | 100.0 | 100.0 | 100.0 | 100.0 |
| | USH1400 | 9 | 4 | 0 | 59 | 93.7 | 94.4 | 69.2 | 100.0 |
| | WSH1400 | 5 | 0 | 4 | 67 | 100.0 | 94.7 | 100.0 | 55.6 |
| | | | | | **Ave.** | **99.2** | **98.6** | **96.2** | **94.4** |
| | H500 | 30 | 0 | 0 | 210 | 100.0 | 100.0 | 100.0 | 100.0 |
| | FB500 | 30 | 0 | 0 | 210 | 100.0 | 100.0 | 100.0 | 100.0 |
| All data | USH500 | 30 | 0 | 0 | 210 | 100.0 | 100.0 | 100.0 | 100.0 |
| | WSH500 | 30 | 0 | 0 | 210 | 100.0 | 100.0 | 100.0 | 100.0 |
| | H1400 | 29 | 0 | 1 | 211 | 100.0 | 99.6 | 100.0 | 96.7 |
| | FB1400 | 29 | 0 | 1 | 211 | 100.0 | 99.6 | 100.0 | 96.7 |
| | USH1400 | 30 | 7 | 0 | 203 | 96.7 | 97.1 | 81.1 | 100.0 |
| | WSH1400 | 24 | 1 | 6 | 215 | 99.5 | 97.2 | 96.0 | 80.0 |
| | | | | | **Ave.** | **99.54±1.45** | **99.16±1.65** | **97.15±7.49** | **96.17±9.76** |

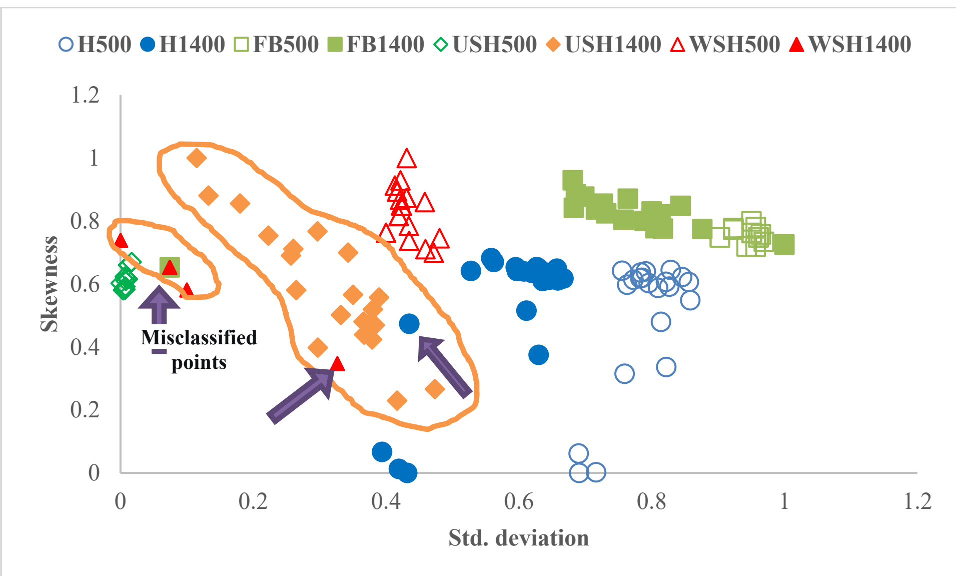


**Fig. 6.** The classification plot of the support vector machine approach.

This phenomenon could stem from either intrinsic overlap in feature distributions among different classes or the presence of outliers in the training dataset.

In a study, the vibration signals in different directions (axial, horizontal, or vertical) and the SVM were used together for mechanical fault diagnosis and online monitoring of the induction motor. The results presented a 96% of hits [24]. Another study employs a multi-sensor system (acoustic, vibration, and current) for the eccentricity and bearing fault diagnosis of induction motors. Data analysis was performed using combined and multi-step methods of LDA, QDA, and SVM. The results showed that the average accuracy was 95% [25].

### *3.4. Models' comparison results*

Comparison of the performance parameters of all three models showed the higher capability of the SVM approach in all cases. The accuracy and sensitivity of the SVM approach were 99.2 and 96.7, respectively. While the QDA approach exhibited the accuracy and the sensitivity of 96.0 and 84.2, respectively, it was the weakest approach (Table 7). The results of the LDA approach revealed that its performance parameters were close to those of the SVM method, with a slight difference. Out of 240 data point, the SVM, LDA, and QDA methods led to 8, 9, and 38 misclassification cases, respectively. Notably, the average performance parameters were the results obtained in the 8 categories, not the mean value of the data. The comparison of LDA, QDA, and SVM was conducted as a validation step to assess the effectiveness of machine learning techniques in classifying defects based on acoustic features.

Our results demonstrate that acoustic-based diagnosis, when paired with proper classifiers, can achieve high accuracy and offer a cost-effective alternative to vibration-based systems in industrial settings.

To ensure a robust evaluation of classifier performance, this study employed both a conventional 70/30 hold-out method and a more rigorous 10-fold cross-validation (CV) approach. Cross-validation provides a significant advantage over simple data splitting by utilizing the entire dataset for both training and validation through multiple iterations, thereby yielding more reliable and generalizable performance estimates while reducing the variance of the results.

A comparative summary of the model performances under both validation schemes is presented in Table 7. While the initial 70/30 split indicated high performance for all models, the cross-validation results provided a more nuanced and trustworthy assessment. The key improvement was observed with the QDA classifier; the CV approach, coupled with pseudo-quadratic discriminant analysis, effectively resolved its initial failure to classify specific fault conditions, which was masked in the simpler split. Furthermore, the CV revealed the superior consistency and stability of the SVM model, as evidenced by its minimal performance variation across different data folds. In contrast, the LDA classifier showed higher performance variability under CV, suggesting its estimates from the single 70/30 split were less reliable.

In conclusion, the cross-validation methodology not only strengthened the credibility of our performance metrics but also confirmed SVM as the most robust and consistent classifier for the task of acoustic-based fault diagnosis, making it the recommended choice for practical industrial applications.

The high diagnostic accuracy demonstrated by the SVM classifier (99.2%) confirms the strong potential of acoustic-based monitoring for industrial implementation. This research provides a practical framework for several applications, including real - time condition monitoring of electromotors, predictive maintenance systems to reduce unplanned downtime, and cost-effective solutions suitable for small-to-medium enterprises using low-cost microphones and standard hardware. Furthermore, the methodology exhibits excellent scalability, being adaptable to other rotating machinery such as pumps, fans, and compressors through model retraining with domain-specific data, and can be integrated with IoT platforms for remote fault diagnosis. The superior performance of the non-linear SVM classifier indicates complex, non-linear relationships in the acoustic data, necessitating curved decision boundaries for optimal fault separation. Conversely, the strong performance of the linear LDA model reveals that a significant linear component also exists, allowing effective class separation through linear discrimination. The initial failure of QDA was not due to methodological weakness but resulted from the "curse of dimensionality"- where limited samples (n=30) made covariance matrices singular. This was resolved using pseudoQuadratic discriminant analysis, demonstrating QDA's effectiveness when numerical stability is ensured. Therefore, SVM emerges as the optimal classifier due to its ability to handle both the linear and non-linear characteristics of the acoustic fault signatures.

## 4. Conclusions

This study successfully demonstrates the effectiveness of acoustic signal analysis combined with machine learning for fault diagnosis in single-phase AC electromotors. The main findings are summarized as follows:

1. Acoustic monitoring effectiveness:

Acoustic signals provide a reliable, non-invasive method for detecting mechanical faults in electromotors, serving as a viable alternative to vibration-based monitoring systems.

2. SVM superior performance:
Among the three classifiers evaluated, Support Vector Machine (SVM) achieved the highest performance with average values of:

- Specificity: 99.5%
- Accuracy: 99.2%
- Precision: 97.1%
- Sensitivity: 96.7%

The superior and most consistent performance of the Support Vector Machine, validated through rigorous 10-fold cross-validation, confirms its high potential for reliable real-time fault diagnosis in industrial environments.

3. Comparative algorithm performance:

- SVM demonstrated the best overall performance
- LDA showed competitive results close to SVM
- QDA exhibited the weakest performance among the three methods

4. Challenging fault conditions:
The WSH1400 class (shaft wear at 1400 rpm) presented the most significant classification challenge due to acoustic signal similarity with the USH1400 and FB1400 classes. This indicates that standard statistical features cannot distinguish between certain mechanical faults (particularly unbalance and shaft wear) that generate similar harmonic responses at high rotational speeds.

5. Industrial applicability:
The proposed method offers:

- Cost-effective solution using low-cost microphones
- Real-time fault detection capability
- Scalability to other rotating machinery
- Potential for predictive maintenance systems

**Table 7.** Comparative Model Performance Evaluation.

| Classifier | Validation method | Specificity | Accuracy | Precision | Sensitivity |
|---|---|---|---|---|---|
| LDA | 70/30 Split | 99.47% ± 1.47 | 98.62% ± 1.77 | 96.61% ± 7.73 | 95.84% ± 9.69 |
| | 10-Fold CV | 99.29% ± 1.19 | 95.00% ± 3.83 | 96.40% ± 6.14 | 95.00% ± 7.13 |
| QDA | 70/30 Split | 97.74% ± 4.16 | 96.02% ± 4.98 | 76.95% ± 33.86 | 84.17% ± 36.96 |
| | 10-Fold CV | 99.76% ± 0.36 | 98.33% ± 2.15 | 98.75% ± 1.89 | 98.33% ± 2.52 |
| SVM | 70/30 Split | 99.54% ± 1.45 | 99.16% ± 1.65 | 97.15% ± 7.49 | 96.17% ± 9.76 |
| | 10-Fold CV | 99.88% ± 0.22 | 99.17% ± 1.76 | 99.37% ± 1.16 | 99.17% ± 1.54 |

6. Future research directions:
- Extension to electrical faults and combined fault conditions
- Implementation of online monitoring systems
- Integration with IoT platforms for remote diagnostics
- Exploration of deep learning approaches for enhanced accuracy

The methodology presents a practical framework for industrial condition monitoring, with SVM emerging as the most robust classifier for acoustic-based fault diagnosis in rotating machinery.

**Data availability statement**

All data generated or analyzed during this study are included in this published article [and its supplementary information files].

**Acknowledgments**

The authors thank all those who helped them in this research, especially the vice chancellor for research and technology of Razi University.

**Conflict of interest**

The above research has no conflict of interest with organizations and individuals.

## References

[1] J. Rafiee, F. Arvani, A. Harifi and M. Sadeghi, "Intelligent condition monitoring of a gearbox using artificial neural network", *MSSP*, Vol. 21, No. 4, pp. 1746-1754, (2007).

[2] M. Zamani, M. Aboonajmi and S. Hassan-Beygi, "Design, development and test of the gearbox condition monitoring system using sound signal processing", *J. Agric. Mach.*, Vol. 6, No. 2, pp. 322-335, (2016). [In Persian]

[3] J. A. Steel and R. L. Reuben, "Recent developments in monitoring of engines using acoustic emission", *J. Strain Anal. Eng. Des.*, Vol. 40, No. 1, pp. 45-57, (2005).

[4] J. J. Saucedo-Dorantes, M. Delgado-Prieto, J.A. Ortega-Redondo, R.A. Osornio-Rios and R.d.J. Romero-Troncoso, "Multiple-fault detection methodology based on vibration and current analysis applied to bearings in induction motors and gearboxes on the kinematic chain", *Shock and Vibration*, Vol. 2016, No. 1, pp. 5467643, (2016).

[5] V. Saxena, N. Chowdhury and S. Devendiran, "Assessment of gearbox fault detection using vibration signal analysis and acoustic emission technique", *J. Mech. Civ. Eng.*, Vol. 7, No. 4, pp. 52-60, (2013).

[6] L. Barelli, G. Bidini, C. Buratti and R. Mariani, "Diagnosis of internal combustion engine through vibration and acoustic pressure non-intrusive measurements", *Appl. Therm. Eng.*, Vol. 29, No. 8-9, pp. 1707-1713, (2009).

[7] A. Glowacz, W. Glowacz, Z. Glowacz and J. Kozik, "Early fault diagnosis of bearing and stator faults of the single-phase induction motor using acoustic signals", *Measurement*, Vol. 113, pp. 1-9, (2018).

[8] E. Ebrahimi and K. Mollazade, "Intelligent fault classification of a tractor starter motor using vibration monitoring and adaptive neuro-fuzzy inference system", *Insight*, Vol. 52, No. 10, pp. 561-566, (2010).

[9] J. Yao, C. Liu, K. Song, C. Feng and D. Jiang, "Fault diagnosis of planetary gearbox based on acoustic signals", *Appl. Acoust.*, Vol. 181, pp. 108151, (2021).

[10] H. Shao, H. Jiang, H. Zhang and T. Liang, "Electric locomotive bearing fault diagnosis using a novel convolutional deep belief network", *ITIE*, Vol. 65, No. 3, pp. 2727-2736, (2017).

[11] G. McLachlan, "Discriminant analysis and statistical pattern recognition", John Wiley & Sons, 2005.

[12] A. Sanaeifar, S. S. Mohtasebi, M. Ghasemi-Varnamkhasti and H. Ahmadi, "Application of MOS based electronic nose for the prediction of banana quality properties", *Measurement*, Vol. 82, pp. 105-114, (2016).

[13] M. Pardo and G. Sberveglieri, "Classification of electronic nose data with support vector machines", *SeAcB*, Vol. 107, No. 2, pp. 730-737, (2005).

[14] A. Sanaeifar, S. S. Mohtasebi, M. Ghasemi-Varnamkhasti and M. Siadat, "Application of an electronic nose system coupled with artificial neural network for classification of banana samples during shelf-life process", *International Conference on Control, Decision and Information Technologies (CoDIT)*, IEEE, pp. 753-757, (2014).

[15] D. M. Sekban, E. U. Yaylacı, M. E. Özdemir, M. Yaylacı and A. Tounsi, "Investigating formability behavior of friction stir-welded high-strength shipbuilding steel using experimental, finite element, and artificial neural network methods", *J. Mater. Eng. Perform.*, Vol. 34, No. 6, pp. 4942-4950, (2025).

[16] J. D. Wu and C. H. Liu, "Investigation of engine fault diagnosis using discrete wavelet transform and neural network", *Expert Syst. Appl.*, Vol. 35, No. 3, pp. 1200-1213, (2008).

[17] K. Salahshoor, M. Kordestani and M.S. Khoshro, "Fault detection and diagnosis of an industrial steam turbine using fusion of SVM (support vector machine) and ANFIS (adaptive neuro-fuzzy inference system) classifiers", *Energy*, Vol. 35, No. 12, pp. 5472-5482, (2010).

[18] J.D. Wu and J.-M. Kuo, "Fault conditions classification of automotive generator using an adaptive neuro-fuzzy inference system", *Expert Syst. Appl.*, Vol. 37, No. 12, pp. 7901-7907, (2010).

[19] E. Ebrahimi, S. Bahrami, N. Astan and M.M. Jalilian, "Application of Neural Networks in Fault Classification of a kind of Clutch Mechanism Retainer", *International Conference on Advanced Mechatronics Solutions*, Springer, pp. 25-32, (2016).

[20] A. Dineva, A. Mosavi, M. Gyimesi, I. Vajda, N. Nabipour and T. Rabczuk, "Fault diagnosis of rotating electrical machines using multi-label classification", *Appl. Sci.*, Vol. 9, No. 23, pp. 5086, (2019).

[21] K. Mahmodi, M. Mostafaei and E. Mirzaee-Ghaleh, "Detection and classification of diesel-biodiesel blends by LDA, QDA and SVM approaches using an electronic nose", *Fuel*, Vol. 258, pp. 116114, (2019).

[22] M. Amarnath, V. Sugumaran and H. Kumar, "Exploiting sound signals for fault diagnosis of bearings using decision tree", *Measurement*, Vol. 46, No. 3, pp. 1250-1256, (2013).

[23] V. Samadi, M. Mostafaei and A. N. Lorestani, "Fault Diagnosis of Electromotor Acoustically Using Machine Learning Approach", *Modares Mech. Eng.*, Vol. 21, No. 8, pp. 563-573, (2021). [In Persian]

[24] L. M. R. Baccarini, V. V. R. e Silva, B. R. de Menezes and W.M. Caminhas, "SVM practical industrial application for mechanical faults diagnostic", *Expert Syst. Appl.*, Vol. 38, No. 6, pp. 6980-6984, (2011).

[25] E. T. Esfahani, S. Wang and V. Sundararajan, "Multisensor wireless system for eccentricity and bearing fault detection in induction motors", *IEEE/ASME Trans. Mechatronics*, Vol. 19, No. 3, pp. 818-826, (2013).